

INDUSTRIAL CROPS AND PRODUCTS

AN INTERNATIONAL JOURNAL





Research article

1

Synthesized high performance UV-cured wood wax oil using Irgacure 2959 modified thistle oil and linseed oil

EI检索

SCI升级版 农林科学1区

SCI基础版 农林科学1区

IF 6.2

Industrial Crops and Products, 15 October 2024

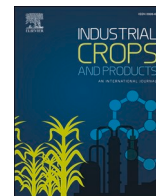
Yijuan Chang, Zhihui Wu

Abstract ▾

Graphical Abstract ▲

Export ▾





Synthesized high performance UV-cured wood wax oil using Irgacure 2959 modified thistle oil and linseed oil

Yijuan Chang^a, Zhihui Wu^{a,b,*}

^a College of Furnishings and Industrial Design, Nanjing Forestry University, Nanjing 210037, China

^b Co-Innovation Center of Efficient Processing and Utilization of Forest Resources, Nanjing Forestry University, Nanjing 210037, China

ARTICLE INFO

Keywords:

UV wood wax oil
Irgacure 2959
Properties
Conversion rate

ABSTRACT

With the reduction of petroleum resources and the intensification of environmental pollution, the development and application of bio-based coatings using renewable resources have become increasingly important in the wood working industry. Wood wax oil is a new bio-based natural coating that provides an environmentally friendly solution for wood preservation. The main challenges related to wood wax oil are slow drying speed and poor liquid resistance. To address this issue, wood wax oil was modified using Irgacure 2959, and the effects of the different concentrations (0, 0.5, 1.0, 1.2 and 1.5 %) of Irgacure 2959 on the properties of ultraviolet (UV) wood wax oil were explored. X-ray photoelectron of spectroscopy analysis indicated that in a wood wax oil film containing 1.2 wt% Irgacure 2959, the C–C and C=O conversion rates are 15.62 % and 25.30 %, respectively. Compared with regular wood wax oil films, the 1.2 % Irgacure 2959 wood wax oil film exhibited a notable 14.2 % decrease in surface roughness. The surface of the UV wood wax oil film exhibits hydrophobic properties, which are positively correlated with its roughness. 1.2 wt% Irgacure 2959 UV-cured wood wax oil with a hardness level of 3 H, an adhesion level of 1, a viscosity of 24.87 s, and a reduction in drying time from 1 h to 20 min. The weather resistance is better than that of the commercial wood wax oil. These findings underscore the potential and versatility of UV wood wax oil, capable of forming a low-roughness and high-gloss wax film on the surface of wooden materials, thus providing an environmentally friendly and non-toxic alternative.

1. Introduction

The application of coatings on wooden surfaces, as commonly observed in wood coatings, serves the dual purpose of safeguarding and enhancing the aesthetic quality of the wood while also sealing the wood's pores (De Meijer, 2001). This protective barrier not only enhances the stability and durability of the wood but also imparts unique attributes such as antibacterial resistance (Deng et al., 2023; Zou et al., 2024), self-healing capabilities (Xia and Yan, 2024), waterproofing (Kapridaki and Maravelaki-Kalaitzaki, 2013), and flame retardancy (Gu et al., 2007), thereby extending the spectrum of functionalities provided to wood (Bulian and Graystone, 2009).

Currently, traditional coatings such as solvent nitrocellulose and polyurethane (PU) coatings have been used as surface coatings for wooden materials (Chattopadhyay and Raju, 2007). However, their use has been restricted in many developed countries owing to their severe environmental pollution and health risks to individuals, as well as harmful effects on the ecosystem (Gan et al., 2023; Li et al., 2009).

Derived from natural extracts, wood wax oil has garnered significant attention both domestically and internationally as an emerging environmentally sustainable coating (Chen et al., 2020). Wood wax oil presents a multitude of merits including profound permeation capability, resistance to moisture (Humar and Lesar, 2013), corrosion (Piao et al., 2022), insects, flames, and ultraviolet resilience (Lesar et al., 2011), accompanied by the absence of deleterious odors (Zhang and Song, 2024). Wood articles subjected to wood wax oil treatment exhibit distinct and authentic grain motifs, a tactually pleasing texture, a surface refraining from film formation (Liu et al., 2024), mitigated tendencies for contraction and expansion, and structural integrity devoid of fractures, warping, or detachment (Ragunathan et al., 2020). Furthermore, the application of wood wax oil entails operational simplicity. Adapting well to an array of climatic conditions, including aridity, humidity, and elevated and diminished temperatures, wood wax oil emerges as an optimal candidate for both interior and exterior embellishment endeavors (Tang et al., 2021). Therefore, the use of sustainable wood wax oil as an environmentally friendly coating has emerged as the preferred

* Corresponding author at: College of Furnishings and Industrial Design, Nanjing Forestry University, Nanjing 210037, China.

E-mail addresses: changyijuan@njfu.edu.cn (Y. Chang), wzh550@sina.com (Z. Wu).

<https://doi.org/10.1016/j.indcrop.2024.118952>

Received 10 March 2024; Received in revised form 6 June 2024; Accepted 7 June 2024

Available online 15 June 2024

0926-6690/© 2024 Elsevier B.V. All rights are reserved, including those for text and data mining, AI training, and similar technologies.

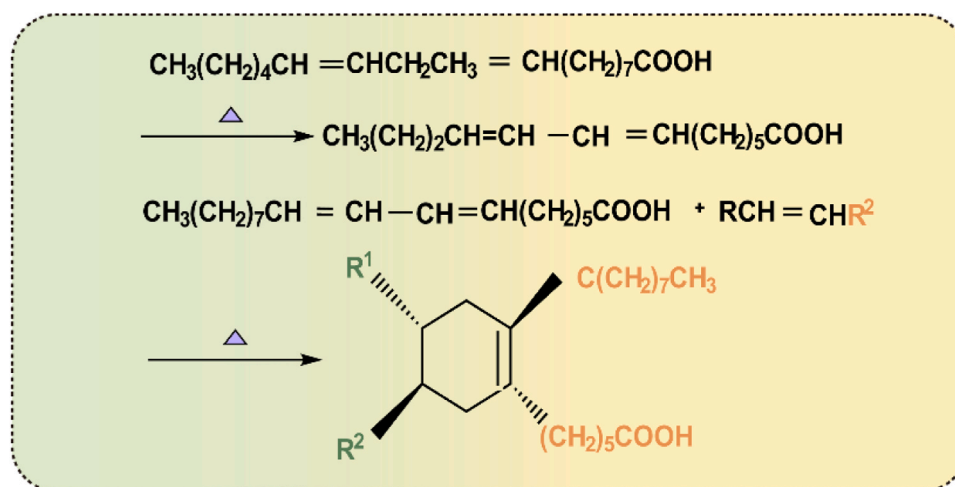


Fig. 1. Synthesis reaction formula of linoleic acid.

solution for addressing the environment and health (Ewa and Björn, 2008).

Wood wax oil primarily comprises drying oils and semi-drying oils (Janesch et al., 2020). Drying oils, characterized by iodine values exceeding 130, readily undergo oxidative polymerization in the presence of air, resulting in elastic and flexible solid films (Wexler, 1964). Semi-drying oil keeps the wax oil in a liquid state. Linseed oil plays a significant role in fast drying and film-forming as a representative drying oil (Nytker et al., 2006). The principal constituents consist of glycerides of unsaturated fatty acids, notably α -linolenic acid and linolenic acid (Schönemann and Edwards, 2011). A study has found that tung oil, whose main component is α -eleostearic acid containing structures such as octadecyl conjugated triene, can form a cured film through auto-oxidation at room temperature. Tung oil-based wood wax oil has good water resistance (Zhang and Song, 2024). However, toxic ingredients such as tung oil ketone acid can cause harm to the human body. Therefore, we introduce environmentally friendly and sustainable thistle oil instead of tung oil (Ullah et al., 2015). In previous study, thistle oil has been utilized in the synthesis of biodiesel, exhibiting fuel properties commensurate with those of mineral diesel (Ullah et al., 2015). The main components of thistle oil include silymarin, linolenic acid, oleic acid, etc. Among them, silymarin is an antioxidant that can reduce the production of free radicals and inhibit lipid peroxidation reactions (Fathi-Achachlouei et al., 2019). Particular emphasis was placed on the significant antioxidative properties exhibited by thistle oil when applied to wood (Singh and Singh, 2012). This application serves to enhance the wood's resistance to atmospheric oxidation. Semi-drying oils (Falkenburg et al., 1948), exemplified by soybean oil and sunflower seed oil with iodine values ranging from 100 to 130, undergo a transition to a colloidal state approximately 7–8 days after application in a thin layer, followed by air drying. Sunflower seed oil and soybean oil contribute to the enhanced flowability of wood wax oil. Functioning as semi-drying oils, they effectively penetrate the pores of wood, safeguarding its internal structure and reinforcing wood preservation

measures. Carnauba wax and beeswax act as film formers and impart a degree of flexibility and hardness to the oil base (de Freitas et al., 2019; Tulloch, 1971). The hardness of carnauba wax exceeds that of beeswax and is employed to regulate the hardness of wood wax oil (Nurul Syahida et al., 2020). It is noteworthy that the synergistic combination of beeswax and carnauba wax often serves to isolate wood products from moisture in the surrounding environment, concurrently enhancing luster and adhesion.

Wood wax oil contains oleic acid and linoleic acid. Under elevated temperature conditions, linoleic acid undergoes isomerization reactions, resulting in the formation of conjugated linoleic acid. When the energy level reaches a specific threshold, the conjugated double bonds engage in Diels–Alder reactions with other unsaturated double bonds, yielding primarily dimeric linoleic acid and minor amounts of trimeric linoleic acid, alongside other polymerization by-products, as shown in Fig. 1. This process serves to enhance the polymerization degree of vegetable oils. Furthermore, other unsaturated fatty acids also exhibit polymerization reactions under high-temperature conditions.

Owing to the presence of antioxidant components such as α -tocopherol and catechol in wood wax oil, these compounds impede the oxidation rate of the oil when exposed to oxygen, resulting in a prolonged drying time for the wood wax oil coating. Therefore, to expedite the drying process, Irgacure 2959 was introduced into the wood wax oil. This photoinitiator can be cured at room temperature or through exposure to UV light. Irgacure 2959, renowned for its efficiency and resistance to yellowing, serves as a photoinitiator for the polymerization reactions of unsaturated pre-polymer systems (Eren et al., 2021). The active hydroxyl groups present in the Irgacure 2959 molecule facilitate interactions through hydrogen bonding (Coimbra et al., 2008). The incorporation of this yellowing-resistant and environmentally friendly Irgacure 2959 into the wood wax oil effectively addresses the challenge of slow curing at room temperature.

We successfully prepared UV wood wax oil, using nitrogen protection during the polymerization process instead of traditional oxygen-



Fig. 2. Wood wax oil raw material.

Table 1
Main components of wood wax oil.

Name	Main ingredients	Function
Linseed oil	α -Linolenic acid $\geq 53\%$	Drying oil
Thistle oil	Oleic acid $\geq 30\%$ Linoleic acid $\geq 40\%$	Drying oil
Sunflower seed oil	Linoleic acid 70.0 %, oleic acid 16 %–20.0 %	Semi-drying oil
Soybean oil	Palmitic acid 6.0–8.0 %, oleic acid 25.0–36.0 %, stearic acid 3.0–5.0 %, linoleic acid 52.0–65.0 %, arachidic acid 0.4–0.1 %, oleic acid 2.0–3.0 %	Semi-drying oil
Beeswax	Palmitate, palmitoleate, and oleate	Auxiliary adjust viscosity
Carnauba wax	Fatty acid methyl ester, polyhydroxyalkanoates	Adjust viscosity
Naphtha	Alkanes 55.4 %, monocyclic alkanes 30.3 %, bicycloalkanes 2.4 %, alkylbenzene 11.7 %	Solvent
Colophony	Abietic acid	Auxiliary

mediated polymerization. This approach enabled the synthesis of transparent composites in a single synthesis step. The wood wax oil upon exposure to UV radiation at room temperature, exhibits exceptional resistance to yellowing. This study focuses on the use of thistle oil as a drying oil instead of traditional toxic tung oil, emphasizing the impact of Irgacure 2959 on the cure time of the wood wax oil. The stability of the UV wood wax oil was assessed through chemical and physical performance evaluations. This innovative approach enhances understanding of the curing kinetics and stability of the UV-cured wood wax oil, offering potential applications in advanced coating technologies.

2. Materials and methods

2.1. Materials

As shown in Fig. 2, the main ingredients of vegetable oil include thistle oil (Panjin Huacheng Pharmaceutical Co., Ltd.) and linseed oil, sunflower oil, and soybean oil (Shanghai McLean Biochemical Technology Co., Ltd.). The main ingredients and functions are as shown in Table 1. The vegetable waxes used were white beeswax (Shanghai McLean Biochemical Technology Co., Ltd.) and carnauba wax (Shandong Yousuo Chemical Technology Co., Ltd.). The additional ingredients used were naphtha (Shandong ChenYu Chemical Co., Ltd.), serve as solvent, hand feel powder SGF-6RM obtained from Shenzhen City Heyan Yuese Plastic Pigment Additive Co., Ltd., and Hunan Jindian Special Pigment Additive Co., Ltd., utilized to increase smooth tactile sensation. Liquid rosin procured from Letong Musical Instrument Co., Ltd., was incorporated to enhance adhesion and impart coloration, while isooctanoic acid acquired from Shanghai McLean Biochemical Technology Co., Ltd., was employed as a drying agent. Irgacure 2959 (Mw: 224.3) was provided by Shanghai Yinchang New Materials Co., Ltd. Basswood (*Tilia*) and walnut (*Juglans spp.*) multilayer board was provided by Zhejiang Shenghua Yunfeng New Materials Co., Ltd. Shanghai, China.

Table 2
UV wood wax oil ingredient list.

Sample	Irgacure 2959 (g)	Linseed oil (g)	Thistle oil (g)	Sunflower oil (g)	Soybean oil (g)	Camaba wax (g)	Beeswax (g)	Rosin (g)	Tactility powder (g)	Isooctanoic acid (g)	Naphtha (g)	Total Weiwei (g)
I2959–0	0	54	18	6.8	6.8	2.7	0.9	18	2.4	12	24	145.6
I2959–0.5	0.8	54	18	6.8	6.8	2.7	0.9	18	2.4	12	24	146.4
I2959–1.0	1.5	54	18	6.8	6.8	2.7	0.9	18	2.4	12	24	147.1
I2959–1.2	1.8	54	18	6.8	6.8	2.7	0.9	18	2.4	12	24	147.4
I2959–1.5	2.25	54	18	6.8	6.8	2.7	0.9	18	2.4	12	24	147.85

2.2. Preparation of UV wood wax oil

(S1) Polymerization of oils and Irgacure 2959. A principal blend of 60.0 % linseed oil and thistle oil in a 3:1 ratio, along with sunflower oil and soybean oil in a 1:1 ratio, was employed. Irgacure 2959 was incorporated at concentrations of 0, 0.5, 1.0, 1.2, and 1.5 %, denoted as I2959–0, I2959–0.5, I2959–1.0, I2959–1.2, and I2959–1.5. The vegetable oil pre-polymerization process involves introducing nitrogen into the reaction system through a three-way valve to isolate air and oxygen. The reaction mixture was subjected to oil bath heating at 110 °C, with stirring at a speed of 600 rpm for a duration of 3 h.

(S2) Wax polymerization. When the temperature descended to 100 °C, a combination of carnauba wax and beeswax in a 3:1 ratio, totaling 6.0 %, was introduced, and the polymerization process was conducted for 1 h.

(S3) Auxiliary agent blending. When the temperature dropped to 60 °C, a formulation consisting of 15.0 % rosin, 2.0 % tactility powder, and 20.0 % naphtha was added. The mixture was stirred for 30 min. After 10.0 % isooctanoic acid was added, stirring continued for an additional 30 min, resulting in the production of an environmentally friendly wood wax oil. The ingredient list of the UV wood wax oil is shown in Table 2.

2.3. Spectroscopy testing and characterization

The composition of the wood wax oil was determined using an ATR method with a VERTEX 80 V infrared spectrometer (Bruker, Germany). The micro-infrared spectra of the walnut I2959–1.2 wood wax oil was tested by LUMOS II FTIRT (Bruker, Germany). The absorbance of the UV wood wax oil was analyzed using a UV–visible (vis) spectrophotometer (U-3900).

2.4. Characterization of physical properties

2.4.1. Color difference

The chromaticity value test was conducted on a basswood multilayer board and the chromaticity value was measured using a SEGT-J portable colorimeter (produced by Zhuhai Tianchuang Instrument Co., Ltd. Zhuhai, China), with color values L_1 , a_1 , and b_1 representing the blank samples, and L_2 , a_2 , and b_2 representing other samples. L represents illuminance, corresponding to brightness, whereas a signifies the range from red to green, and b denotes the range from blue to yellow. The color difference calculation formula is as follows (1) (Coronel-Aguilera and San Martín-González, 2015).

$$\Delta E \text{ (color difference)} = [(\Delta L^*)^2 + (\Delta a^*)^2 + (\Delta b^*)^2]^{1/2} \quad (1)$$

where $\Delta L^* = L_1 - L_2$, $\Delta a^* = a_1 - a_2$, and $\Delta b^* = b_1 - b_2$.

2.4.2. Gloss

The wood wax oil was applied onto a 150 mm × 150 mm black glass substrate, and the gloss of the coating at a 60° angle was measured using an HG268 intelligent gloss meter (3nh Technology Co., Ltd., Shenzhen) in accordance with the GB/T 4893.6–2013 “Furniture Surface Coating Physicochemical Properties Testing–Part 6: Gloss Measurement Method.”

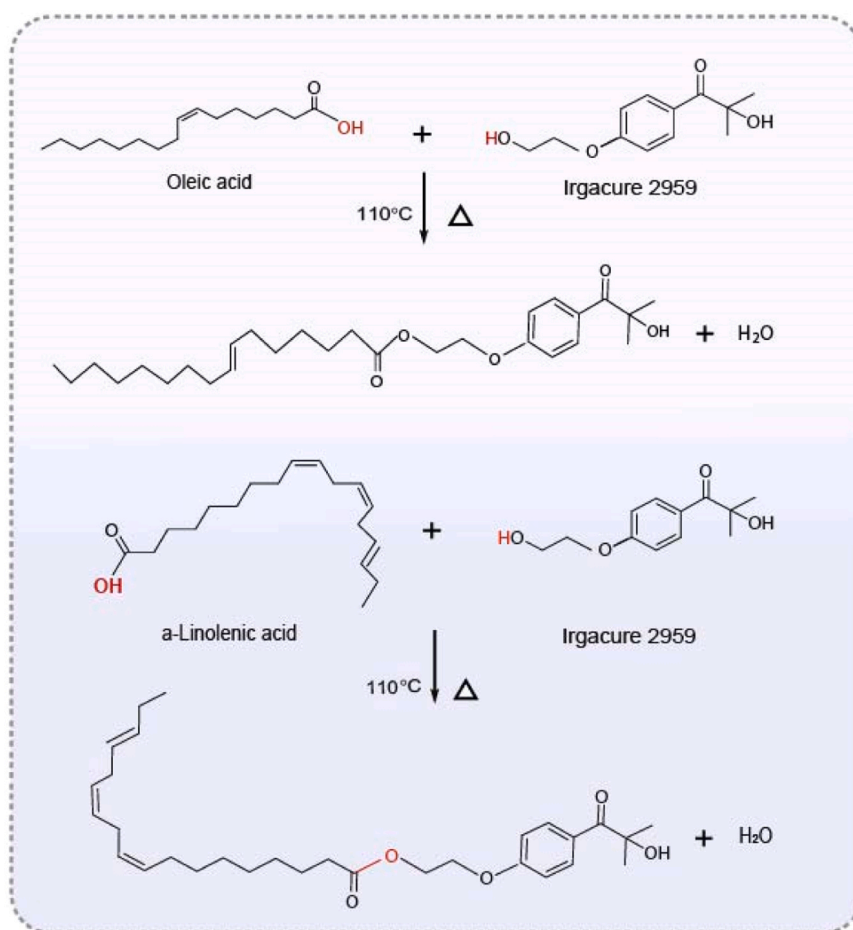


Fig. 3. Reaction mechanism of UV wood wax oil.

2.4.3. Roughness

The basswood substrates were polished with 1000 grit sandpaper, and then coated with UV wood wax oil to test the roughness. The roughness of the basswood wax oil coating was tested using a JB-4 C precision roughness tester (Shanghai Taiming Optical Instrument Co., Ltd.).

2.4.4. Contact angle

The water contact angles (WCAs) of the walnut wood wax oil surfaces were tested using a DSA100S droplet shape analyzer (KRÜSS, Germany). These surfaces were cut into strips with the width of approximately 1.0 cm. The WCAs at the different elapsed time (0 s, 5 s, 10 s, and 20 s) were recorded at five positions, with 5 μ L water droplets.

2.4.5. Viscosity

The viscosity of the wood wax oil was determined according to the GB/T 1723–1993 “Determination of Viscosity of Coatings” for coating viscosity measurement, using a KU-4 viscometer.

2.4.6. Drying time

The drying time of the walnut wood wax oil film was evaluated under 1 kW high-pressure mercury lamp curing, in compliance with GB/T 1728–2020 “Method for Determining the Drying Time of Paint Films and Putty Films.”

2.4.7. Gel content

Initially, 1.0 g of wood wax oil was individually weighed and placed within a glass container, denoted as m_1 . Subsequently, upon complete solidification, the combined weight of the glass container and the wood

wax oil was determined as m_2 . The ratio of the mass of the residue after drying to the mass of the sample is the gel content. The gel content of the wood wax oil was then computed using Eq. (2):

$$\text{Gel content (\%)} = \frac{m_2}{m_1} \times 100 \quad (2)$$

2.4.8. Hardness

The hardness of the paint film was determined according to the GB/T 6739–2006 “Pencil Hardness Test for Paints and Varnishes,” pencils of varying hardness from 6H to 6B were employed. A higher B number indicates a darker and softer pencil, whereas a higher H number indicates a lighter and harder pencil. HB represents an intermediate hardness level. The pencil, held at an angle of approximately 45° to the paint film surface, was pushed forward across the coating under a 1.0 kg load at a speed of 1.0 cm/s. The maximum hardness of the pencil at which the coating remained undamaged was recorded as the hardness of the wood wax oil film.

2.4.9. Adhesion

The adhesion of the coating was determined in accordance with the GB/T 4893.4–2013 “Furniture Surface Coating Physicochemical Properties Testing – Part 4: Cross-Cut Test for Adhesion.” The QFH-HG600 paint film cross-cut tester was used to assess the adhesion of the walnut coating. After the cross-cut was made, the area was brushed to remove any loose fragments, and then 3M tape was applied. It was rubbed back and forth with a finger to ensure secure adhesion, and then the tape was swiftly peeled off. The smoothness of the cut edges and any fragment detachment from the tape were observed and rated according to the provided chart. Coating damage was categorized into six levels,

Table 3

Wood wax oil infrared absorption spectrum section.

Thistle oil	Linseed oil	Wood wax oil	Corresponding functional groups
3008	3009		C=C-based stretching vibration
2987	2987		CH ₃
2920	2923	2920	CH ₃
2854	2855	2854	CH ₂
1743	1742	1743	C=O
1650		1650	C=C
1455	1454	1455	C-H
1156	1158	1156	C-O
1104	1103	1091	C=O
989	989	989	C-C
721	721	721	-CH ₂
590	590	590	CH base swing vibration

ranging from 0 (strongest adhesion) to 5 (weakest adhesion). If the coating's intact rate exceeded 70.0 %, it was considered good; otherwise, it was deemed damaged.

2.5. Thermal stability

Thermogravimetric (TG) analysis measurements of UV-cured wood wax oil films were performed on a TG 209 from TA Instruments to study the thermal stability of the samples. The temperature ramp was maintained at a controlled rate of 10 °C/min with a flow rate of 20 mL/min, within a heating range spanning from room temperature to 700 °C.

2.6. Cold-resistant liquid performance

The testing was conducted in accordance with the provisions of GB/T

4893.1 "Test of Surface Coatings of Furniture – Part 1: Determination of Surface Resistance to Cold Liquids." The test durations were as follows: 24 h in grade 3 water, 48 h in a (1 ± 20) acetic acid solution, and 1 h in a 5 % (mass fraction) sodium carbonate solution. The chromaticity values and gloss of walnut wood before and after liquid resistance were tested.

2.7. Weather resistance testing

The weather resistance testing of the wood wax oil coating on the basswood surface was assessed according to GB/T 1865–2009, UVA-340 lamps, and an irradiance of 8 W/m². (Chen et al., 2022). These boards are placed in a constant temperature and humidity box with a temperature of 40 °C and a humidity of 60 % for 4 h, and then placed in a UV box for 4 h. This whole process is regarded as a cycle. A total of 8 aging cycles were performed, with a total aging time of 64 h. One panel was retained as a control sample and stored at room temperature, shielded from moisture and light. To ensure uniform exposure, the panels were rearranged at intervals not exceeding 4 h. After every 8 h of aging exposure, chromaticity values and gloss in the test samples were evaluated. The color difference was calculated according to Eq. (1). The loss of gloss after aging resistance was calculated according to the formula (3).

$$L(\%) = \frac{G_1 - G_2}{G_1} \times 100 \quad (3)$$

L (%) is the gloss loss rate, G₁ is the gloss before weather resistant, and G₂ is the gloss after weather resistant.

The above tests were conducted three times on each sample, and the average value was taken.

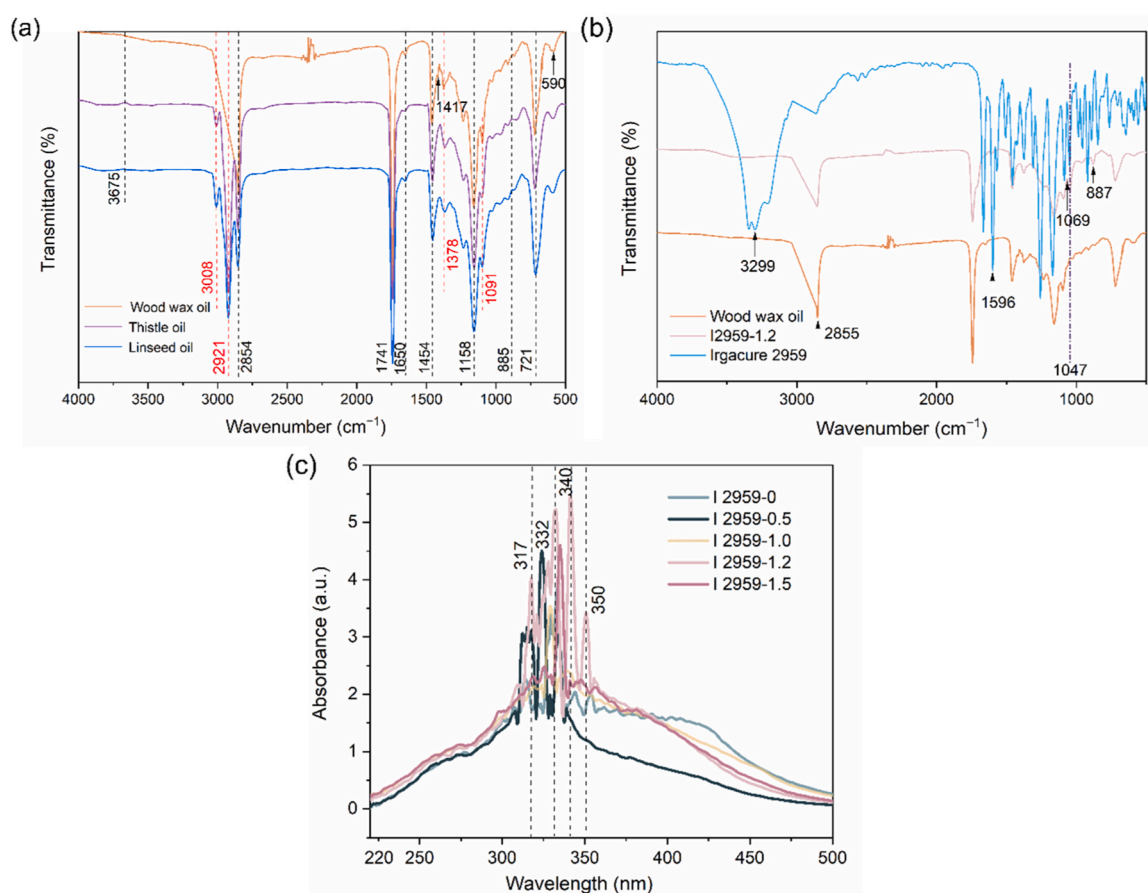


Fig. 4. (a) Infrared spectrum of wood wax oil and raw materials, (b) UV wood wax oil infrared spectroscopy, and (c) the absorbance of wood wax oil with different concentrations of Irgacure 2959.

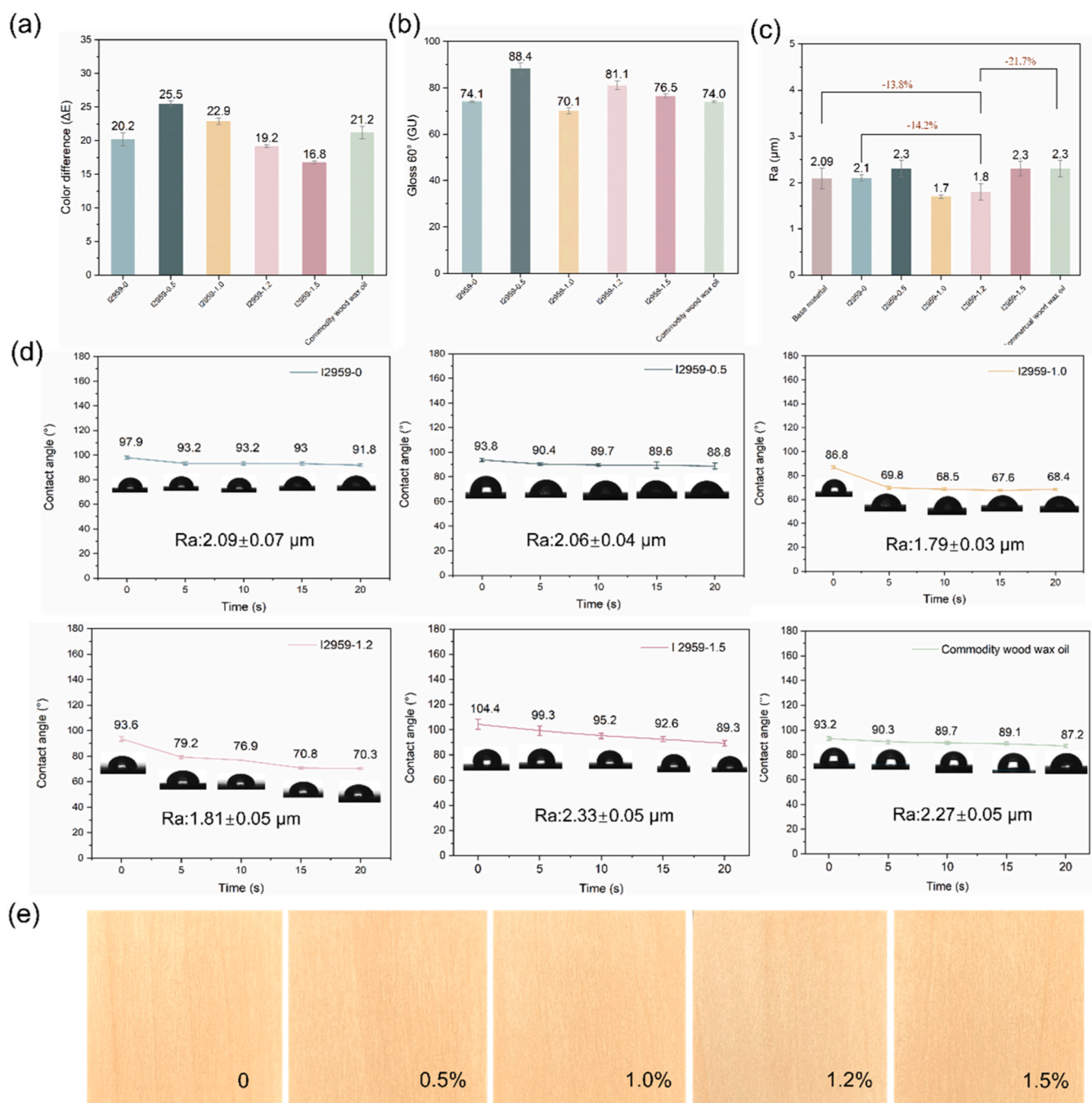


Fig. 5. (a) Color difference, (b) gloss, (c) roughness values of wood wax oil, (d) contact angle and (e) basswood with different Irgacure 2959 concentrations.

3. Results and discussion

3.1. Synthesis of UV wood wax oil

Fig. 3 depicted the structural formula illustrating the reaction between Irgacure 2959, oleic acid, and α -linolenic acid. The active hydroxyl group of the Irgacure 2959 forms ester bonds with the carboxyl groups present in oleic acid and α -linolenic acid, initiating an esterification reaction that results in the formation of polymers and water (Eren et al., 2021). The generated water can be effectively separated using an oil-water separator.

3.2. Infrared spectroscopic and UV-vis spectra analysis

The characteristic peaks of the components of the wood wax oil were shown in Table 3. As shown in Fig. 4(a), after subjecting oil-wax raw materials, primarily consisting of linseed oil and thistle oil, to a high-temperature pre-polymerization process at 110 °C, pronounced changes in the vibrational spectra of specific functional groups were observed. Evidently, the C-H stretching vibrations on the C=C bonds at 3008 cm^{-1} gradually diminished with the high-temperature polymerization of linseed oil and thistle oil. Simultaneously, the O-H stretching vibrations at 2921 cm^{-1} also vanished. This phenomenon signified a reduction in the active hydrogen concentration of the resulting wood wax, indicative of a polymerization reaction occurring within the plant oil-wax system (Peng et al., 2020). Furthermore, a decreasing trend in

the O–H stretching vibrations at 3675 cm^{-1} was noted, likely attributed to the hydrolysis reaction of ester bonds in linseed oil. In parallel, an enhanced trend was observed in the stretching vibrations of the C–O–C ether bonds at 1091 and 1378 cm^{-1} , indicating the occurrence of polymerization reactions within the plant oil–wax system (Schönemann and Edwards, 2011). Simultaneously, the C–H of α -linolenic acid, represented by the emergence of the C=C bond at 1417 cm^{-1} , and the –CH functional group at 590 cm^{-1} displayed weakened vibrational peaks following the oil polymerization process (Rosu et al., 2018). It is noteworthy that Irgacure 2959 needs to undergo polymerization in conjunction with oleic acid and α -linolenic acid, otherwise, following the polymerization of oleic acid and α -linolenic acid, Irgacure 2959 remains unreacted.

The esterification reaction between Irgacure 2959, oleic acid, and α -linolenic acid resulted in the formation of esters and water. In this reaction, the hydroxyl group in Irgacure 2959 reacted with the carboxyl groups in oleic acid and α -linolenic acid under high-temperature anaerobic conditions. In Fig. 4(b), the peak at 3299 cm^{-1} corresponds to the –OH group in the Irgacure 2959. After the esterification reaction, the –OH peak diminishes, and a new peak at 1047 cm^{-1} arises, indicating the formation of C–O bonds. This observation confirmed the esterification reaction between oleic acid, α -linolenic acid, and Irgacure 2959. The successful preparation of the UV wood wax oil was thus inferred. Fig. 4(c) presented the UV absorbance spectrum of the UV wood wax oil, spanning the absorption wavelengths from 220 to 500 nm. Peaks with elevated absorbance in the spectrum are typically correlated with absorption peaks of specific compounds. In this context, the heightened absorbance with I2959–1.2 aligns with the complete reaction of Irgacure 2959 with oleic acid and α -linolenic acid. The UV spectrum of the I2959–1.2 exhibited five prominent absorption bands in the range of 310–350 nm in the infrared spectrum, originating from electronic transitions of the acyl groups. The most intense absorption peak occurred at 340 nm, attributed to $n \rightarrow \pi^*$ electron transitions in the carbonyl and carboxyl groups of the R-band, accompanied by a redshift.

3.3. Physical properties of UV-cured wood wax oil

In Fig. 5(a), the color difference of basswood UV-cured wood wax oil coating calculations was performed, in comparison with the blank substrate. All UV-cured wood wax oil exhibited a significantly greater color difference, enhancing the warmth of the wood, whereas the I2959–1.5 wood wax oil displayed the least color difference. In Fig. 5(b), the gloss of I2959–1.2 was observed to be lower than that of I2959–0.5, and its gloss is higher than that of commercial wood wax oil. Fig. 5(c) revealed a 14.2 % reduction in roughness for I2959–1.2 compared with I2959–0 and a remarkable 13.8 % reduction relative to the substrate. Furthermore, the roughness was 21.7 % lower than that of the commercial wood wax oil, indicating that the UV-cured wood wax oil effectively filled the surface pores of the substrate, covering exposed cell lumens and resulting in a highly cross-linked, smooth, and stable film. (Varganici et al., 2021)

The water contact angle and roughness of six surfaces were presented in Fig. 5(d). The results demonstrated that the wood wax oil coating exhibited a certain degree of wettability, with the contact angle of I2959–1.2 approaching 90° , and decreased with increasing contact time. The initial WCA for I2959–0 was 97.9° at 0 s and 91.8° at 20 s, the WCA of I2959–1.0 at 0 s and 20 s were 86.8 and 68.4° respectively. The initial WCA of I2959–1.5 was 104.4° and the WCA at 20 s was 89.3° . These results indicated that the WCAs of surfaces with different photo-initiator were significantly different. And a positive correlation was observed between the surface roughness (Ra) value and the WCA. (Zhang et al., 2023) The Ra values of I2959–0, I2959–0.5, I2959–1.0, I2959–1.2, and I2959–1.5 were 2.09 ± 0.07 , 2.06 ± 0.04 , 1.79 ± 0.03 , 1.81 ± 0.05 , $2.33 \pm 0.05\text{ }\mu\text{m}$, respectively. The surface contact angle and roughness in this study were comparable to those of commercial wood wax oil.

Table 4

UV wood wax oil physical properties.

Sample	Viscosity (S)	Gel content (%)	Drying time (min)	Hardness	Adhesion
I2959–0	48.81 ± 0.76	99.57 ± 1.01	49.0 ± 0.5	4 H	1
I2959–0.5	45.88 ± 4.11	99.58 ± 1.21	45.0 ± 0.4	3 H	1
I2959–1.0	27.87 ± 0.04	99.59 ± 1.35	35.0 ± 0.3	3 H	1
I2959–1.2	24.87 ± 0.47	99.31 ± 1.15	20.0 ± 0.2	3 H	1
I2959–1.5	23.27 ± 1.59	99.45 ± 1.31	30.0 ± 0.3	3 H	1

As illustrated in Fig. 5(e), the application of basswood coatings with varying concentrations of Irgacure 2959 was observed to enhance both the hue and gloss of the basswood substrate. The modulation of color intensity and surface luminosity was attributed to the controlled incorporation of the Irgacure 2959 reagent into the basswood coating matrix. This nuanced manipulation of the Irgacure 2959 concentration serves to impart distinctive optical characteristics to the basswood, thereby contributing to an augmented visual appeal. The findings presented in Fig. 5(e) underscored the significant impact of Irgacure 2959 concentrations on the aesthetic attributes of basswood coatings, providing valuable insights for the optimization of wood finishing processes.

As shown in Table 4, the viscosity of the UV wood wax oil decreased proportionally with the increase in Irgacure concentration. This phenomenon arises owing to the reaction between Irgacure 2959, oleic acid, and α -linolenic acid, resulting in the formation of new esters and water. Consequently, this reaction led to a reduction in the viscosity of the wood wax oil. Wood wax oil with high gel content exhibited longer drying times, whereas oil with low gel content had shorter drying times. The gel content of the samples was consistently high, all exceeding 99.0 %. I2959–1.2 exhibited the shortest curing time, thereby demonstrating the highest curing efficiency among the tested formulations. The curing time of the wood wax oil varied with the absence or presence of various concentrations of Irgacure 2959. Notably, the I2959–1.2 wood wax oil exhibited a curing time of 20 min, whereas the other samples required 30 min for solidification. This discrepancy suggested that I2959–1.2 imparted heightened UV absorbance to the wood wax oil, indicating its maximum absorption capacity in the UV–vis absorption spectrum. The coating hardness of the UV-cured wood wax oil was notably superior, measuring at 3–4 H, with consistently high adhesion levels rated at grade 1.

3.4. Thermal stability of UV-cured wood wax oil

The TG and DTG of the UV-cured wood wax oil were presented in Fig. 6. Fig. 6(a) showed that I2959–1.2 underwent pyrolysis at the latest stage, achieving a thermal decomposition efficiency of 82.86 % between 244°C and 490°C . Conversely, I2959–0.5 began pyrolysis at the earliest stage. These results indicated that the wood wax oil coating of I2959–1.2 possessed the highest thermal stability. Fig. 6(b) presented that the I2959–1.2 wood wax oil coating exhibited the maximum weight loss rate at 420.7°C . This demonstrated that UV wood wax oil could withstand the test of high temperature and had the potential to be used as a coating for outdoor wood products. (He et al., 2019)

3.5. Chemical structure and composition

In Fig. 7(a), the C1s X-ray photoelectron of spectroscopy (XPS) analysis revealed the presence of C–C, C–O, and C=O bonds in the I2959–1.2 UV-cured wood wax oil coating, with binding energies of 284.8, 286.4, and 289.0 eV , respectively (Giesbers et al., 2013). It is worth noting that the presence of C=O observed in XPS C1s spectra

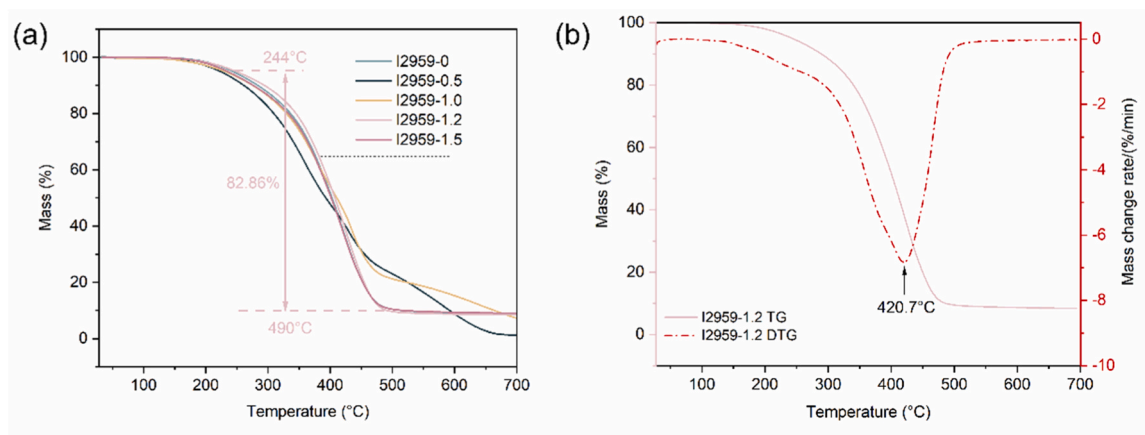


Fig. 6. TG and DTG curves of UV-cured wood wax oil.

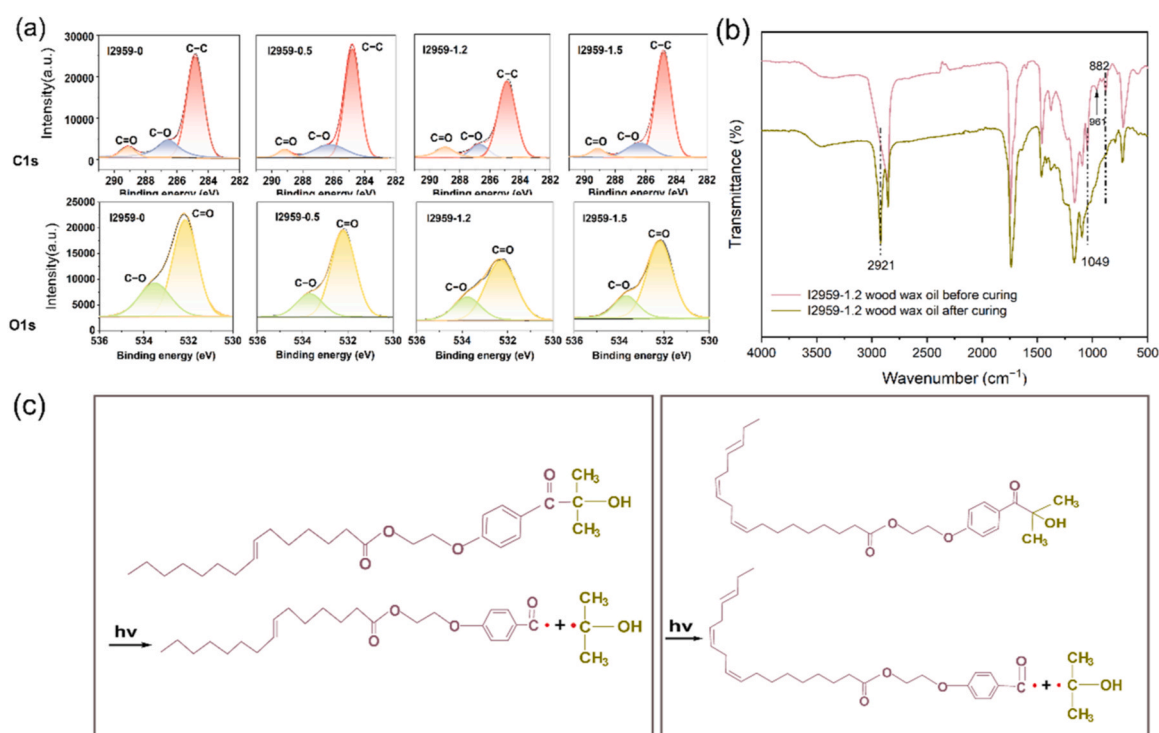


Fig. 7. (a) UV-vis spectra of UV-cured wood wax oil C1s and O1s, (b) I2959-1.2 wood wax oil before and after curing, and (c) curing mechanism of UV wood wax oil.

Table 5
C and O conversion rates of UV-cured wood wax oil.

Sample	C1s	C-C conversion rate (%)	O1s	C=O conversion rate (%)
I2959-0	33,027.87		26,353.53	
I2959-0.5	32,890.00	0.42	22,839.52	13.33
I2959-1.2	27,868.54	15.62	19,685.37	25.30
I2959-1.5	33,787.35	-2.30	22,905.97	13.08

indicated that only a portion of C=O in the UV wood wax oil was converted to $\bullet\text{C}-\text{O}\bullet$.

The O1s XPS spectrum analysis revealed the existence of C=O and C-O bonds in the wood wax oil coating, with binding energies of 531.5–532 and 533 eV, respectively (Schindler et al., 2009). The integrated areas of C and O of I2959-1.2 were significantly reduced. Conversely, after the reaction with 1.5 % I2959, an increase in the

integrated areas of C and O was noted. This observation suggested that during the curing process of the UV-cured wood wax oil, I2959-1.2 exhibited the highest participation in the curing process, leading to the most significant decrease in the concentration of C and O. These outcomes aligned with the observed maximum UV absorbance in Fig. 4(c), establishing a congruent relationship between the Irgacure concentration and the transformative processes (Eren et al., 2021).

The conversion rates of C-C and C=O fractions in the wood wax oil with different concentrations of Irgacure 2959 were shown in Table 5. Notably, the I2959-1.2 wood wax oil exhibited the highest conversion rates for both C-C and C=O functionalities, registering at 15.62 % and 25.30 %, respectively. Fig. 7(b) represented the emergence of saturated CH_2 functionalities at 2921 cm^{-1} , CH functionalities at 882 cm^{-1} , and C-H C=C-H functionalities at 961 cm^{-1} observed in the cured state of the UV-cured wood wax oil. The disappearance of CH bonds after curing further corroborated the successful solidification of the UV-cured wood wax oil. Fig. 7(c) illustrated the curing mechanism of the UV wood wax

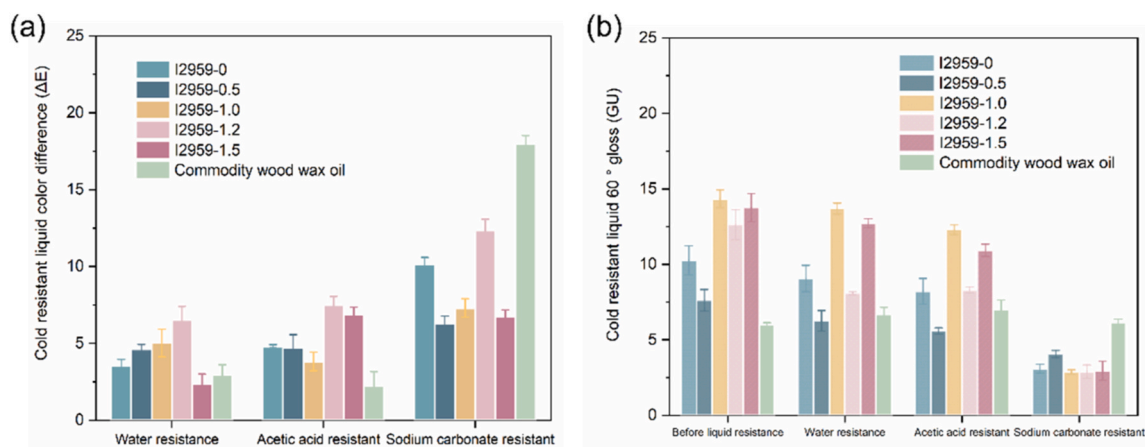


Fig. 8. (a) Color difference and (b) gloss of wood wax oil before and after cold liquid resistance.

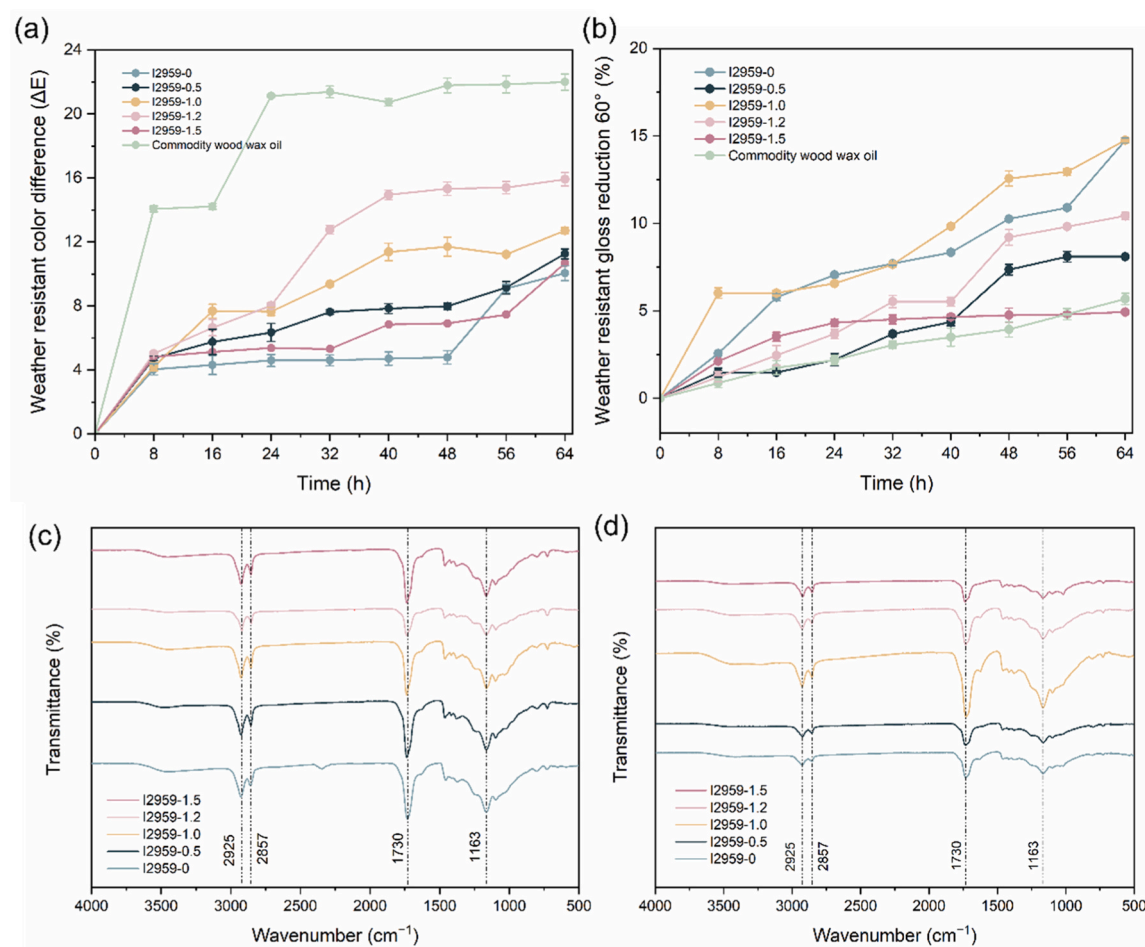


Fig. 9. (a) Weathering color difference of UV-cured wood wax oil, (b) UV-cured wood wax oil weathering gloss loss rate (c) infrared spectrum of UV-cured wood wax oil before weathering, (d) infrared spectrum of UV-cured wood wax oil after weathering.

oil. The esterified wood wax absorbed light energy, leading to the decomposition and generation of polymer radicals and α -hydroxyisopropyl radicals, both of which served as initiators for polymerization, with the latter exhibiting greater reactivity in the reaction process.

3.6. Analysis of cold liquid resistance of UV-cured wood wax oil

The gloss and color difference before and after exposure to cold-

resistant liquid for the wood wax oil were depicted in Fig. 8. As illustrated in Fig. 8(a), there was a significant color difference observed in the commercial wood wax oil after exposure to sodium carbonate, whereas the color difference stability of the wood wax oil studied herein surpassed that of the commercial counterpart. The Fig. 8(b) showed that I2959-1.0 and I2959-1.5 wood wax oils exhibited higher gloss before liquid resistance testing, maintaining elevated levels even after exposure to water and acetic acid. However, a noticeable decline in gloss was

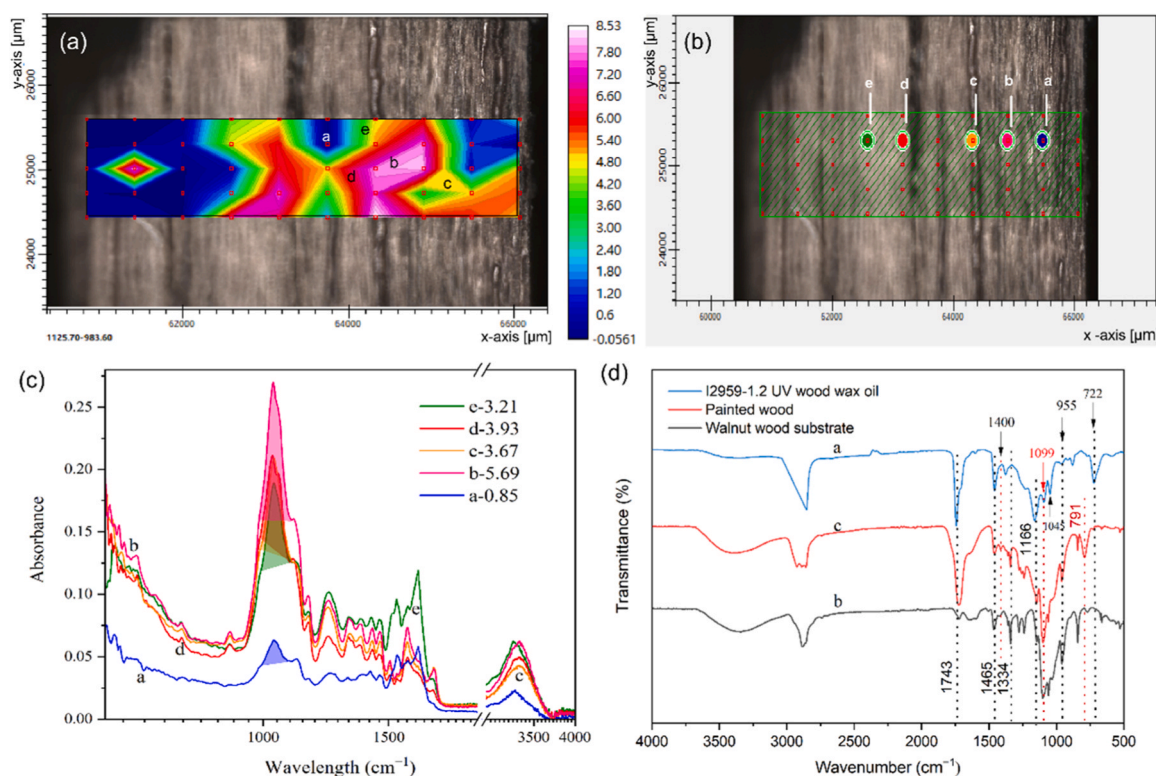


Fig. 10. (a) U-FTIR analysis of I2959-1.2, (b) microscopic infrared selected points, (c) I2959-1.2 integral areas, and (d) ATR-FTIR spectra I2959-1.2 wood wax oil and substrate.

observed after exposure to of the samples to sodium carbonate, accompanied by a gradual increase in color difference. The gloss of I2959-1.2 wood wax oil remained relatively consistent before and after water and acetic acid resistance. Considering both gloss and color difference comprehensively, the I2959-1.2 wood wax oil demonstrated a more stable performance in cold-resistant liquid durability.

3.7. Analysis of weather resistance performance of UV-cured wood wax oil

The results of 64 h weather resistance test on the UV wood wax oil were illustrated in Fig. 9. Fig. 9(a) indicated that under weather resistance, Irgacure 2959 exhibited an augmented capacity for weather resistance, resulting in reduced and stabilized resistance to color differences. Fig. 9(b) showed that the gloss loss rate of the wood wax oil coatings with different concentrations of Irgacure 2959 increases or remains stable over time, and I2959-1.2 was lower than the gloss loss rate of commercial wood wax oil, indicating that the UV-cured wood wax oil coatings showed a comparable level of gloss after weathering. Fig. 9(c) was the infrared spectrum before weathering, and Fig. 9(d) was the infrared spectrum after weathering. The emergence of saturated CH₂ functionalities at 2921 cm⁻¹ and 2857 cm⁻¹, 1730 cm⁻¹ is C=O and 1163 cm⁻¹ is C-O, no new chemical bonds appear or disappear in the UV wood wax oil before and after weathering. The results showed that no chemical changes occur in the UV-cured wood wax oil before and after weathering.

3.8. Wood wax oil coating microscopic infrared

The micro-infrared spectra of the I2959-1.2 wood wax oil was presented in Fig. 10. The corresponding features labeled as “a,” “b,” “c,” “d,” and “e” exhibit a consistent pattern. In Fig. 10 (a), the magenta-colored regions indicated the highest penetration, with the color gradient on the chart representing a decreasing concentration of the

wood wax oil from top to bottom. The infiltration of the wood wax oil from right to left was illustrated in Fig. 10 (b), and the integral areas at different locations were depicted in Fig. 10 (c). Larger integral areas signify greater penetration, with zone b exhibiting the maximum infiltration. Given the heterogeneous nature of wood as a material, the permeation of the wood wax oil within it appeared to be characterized by irregular and non-uniform patterns. The infrared spectra depicting the interaction between the substrate and the wood wax oil were presented in Fig. 10 (d). The absorption peak at 722 cm⁻¹ corresponded to the bending vibration of the cis-C=C bond in α -linolenic acid or oleic acid present in linseed oil (Arminger et al., 2020). The prominent C-H vibration peak at 791 cm⁻¹ was observed in spectrum c, whereas the C-O absorption at 1045 cm⁻¹ in the substrate disappeared, indicating a reaction between the wood wax oil and lignin in the substrate. The peak at 1060 cm⁻¹ represented the stretching vibration of C-O in wood hemicellulose, whereas that at 1099 cm⁻¹ corresponded to the flexural vibration of C-O. The spectrum of the coated substrate (spectrum c) surpassed those of spectra a and b, suggesting a substantial reaction between hemicellulose and wood wax oil. The signal at 1166 cm⁻¹ was attributed to the stretching vibration of C-O-C (Ou et al., 2015; Rosu et al., 2018). The absorption peaks of the coated wood at 1400 and 1465 cm⁻¹ were enhanced. The peak at 1465 cm⁻¹, arising from the anti-symmetric bending vibration of -CH₂, exhibited a decrease in intensity²⁰. The absorption peak at 1743 cm⁻¹ corresponded to the stretching vibration of C=O (Chen et al., 2011) (Pandey, 1999; Traoré et al., 2016). Spectrum c significantly surpassed spectra a and b, indicating vibrational changes. This suggested that the carboxyl groups in the fatty acid chains of the wood wax oil undergo esterification reactions with the hydroxyl groups in the substrate's hemicellulose and lignin, leading to the formation of new C=O bonds (Schwanninger et al., 2004) (Pandey and Pitman, 2003; Peng et al., 2020).

4. Conclusions

In this study, we presented a UV-cured wood wax oil synthesized using Irgacure 2959. The introduction of an Irgacure at a concentration of 1.2 % in the wood wax oil enhances the color and gloss of the wood material. In comparison with regular wood wax oil films, the I2959–1.2 UV-cured wood wax oil exhibited a notable 14.2 % reduction in surface roughness, the surface of the UV wood wax oil film exhibits hydrophobic properties, which are positively correlated with its roughness. I2959–1.2 UV-cured wood wax oil achieving a hardness level of 3 H, an adhesion level of 1, a viscosity of 24.87 s, and a drying time of 20 min. I2959–1.2 results in heightened light absorption by the wood wax oil, maximizing its absorption capacity. At a 1.2 % concentration of Irgacure 2959, the C–C and C=O conversion rates were 15.62 % and 25.30 %, respectively, representing conversion rates higher than those of other concentrations. The weather resistance is better than that of commercial wood wax oils. In addition, the UV-cured wood wax oil undergoes esterification reactions with the hydroxyl groups in the hemicellulose and lignin of the walnut substrate, forming new C=O bonds. The resistance to cold liquids remains stable, and the aging resistance surpasses that of commercial wood wax oils.

Funding

This work was funded by the National Key Research and Development Program (nos. 2016YFD0600704, 2018YFD0600304, and 2023YFD2201501) and the Postgraduate Research and Practice Innovation Program of Jiangsu Province (grant no. KYCX23_1195).

CRediT authorship contribution statement

Yijuan Chang: Writing – review & editing, Writing – original draft, Resources, Methodology, Investigation, Formal analysis, Data curation. **Zhihui Wu:** Writing – review & editing, Validation, Supervision, Funding acquisition.

Declaration of Competing Interest

The author declared that they have no conflicts of interest to this work. We declare that we do not have any commercial or associative interest that represents a conflict of interest in connection with the work submitted.

Data availability

Data will be made available on request.

References

- Arminger, B., Jaxel, J., Bacher, M., Gindl-Altmutter, W., Hansmann, C., 2020. On the drying behavior of natural oils used for solid wood finishing. *Prog. Org. Coat.* 148, 105831.
- Bulian, F., Graystone, J.A., 2009. Chapter 1 - Markets for Wood and Wood Coatings. In: Bulian, F., Graystone, J.A. (Eds.), *Wood Coatings*. Elsevier, Amsterdam, pp. 1–14.
- Chattopadhyay, D.K., Raju, K.V.S.N., 2007. Structural engineering of polyurethane coatings for high performance applications. *Prog. Polym. Sci.* 32, 352–418.
- Chen, Y., Liu, R., Luo, J., 2022. Enhancing weathering resistance of UV-curable coatings by using TiO₂ particles as filler. *Prog. Org. Coat.* 169, 106936.
- Chen, C.J., Luo, J.J., Huang, X.P., Zhao, S.K., 2011. Analysis on cellulose crystalline and FTIR spectra of *Artocarpus heterophyllus* Lam wood and its main chemical compositions. *Adv. Mater. Res.* 236–238, 369–375.
- Chen, J., Wang, Y., Cao, J., Wang, W., 2020. Improved waterrepellency and dimensional stability of wood via impregnation with an epoxidized linseed oil and carnauba wax complex emulsion. *Forests* 11, 271.
- Coimbra, P., Fernandes, D., Ferreira, P., Gil, M.H., de Sousa, H.C., 2008. Solubility of Irgacure® 2959 photoinitiator in supercritical carbon dioxide: experimental determination and correlation. *J. Supercrit. Fluids* 45, 272–281.
- Coronel-Aguilera, C.P., San Martín-González, M.F., 2015. Encapsulation of spray dried β -carotene emulsion by fluidized bed coating technology. *LWT - Food Sci. Technol.* 62, 187–193.

- De Meijer, M., 2001. Review on the durability of exterior wood coatings with reduced VOC-content. *Prog. Org. Coat.* 43, 217–225.
- Deng, J., Huang, N., Yan, X., 2023. Effect of composite addition of antibacterial/ photochromic/self-repairing microcapsules on the performance of coatings for medium-density fiberboard. *Coatings* 13, 1880.
- Eren, T.N., Karikisz, N., Demirci, G., Tuncel, D., Okte, N., Yagci Acar, H., Avci, D., 2021. Irgacure 2959-functionalized poly(ethyleneimine)s as improved photoinitiators: enhanced water solubility, migration stability and visible-light operation. *Polym. Chem.* 12, 2772–2785.
- Ewa, J.M., Björn, S., 2008. Wood cell walls: biosynthesis, developmental dynamics and their implications for wood properties. *Curr. Opin. Plant Biol.* 11, 293–300.
- Falkenburg, L.B., DeJong, W.M., Handke, D.P., Radlove, S.B., 1948. Isomerization of drying and semi-drying oils: the use of anthraquinone as a conjugation catalyst. *J. Am. Oil Chem. Soc.* 25, 237–243.
- Fathi-Achachlouei, B., Azadmard-Damirchi, S., Zahedi, Y., Shaddel, R., 2019. Microwave pretreatment as a promising strategy for increment of nutraceutical content and extraction yield of oil from milk thistle seed. *Ind. Crops Prod.* 128, 527–533.
- de Freitas, C.A.S., de Sousa, P.H.M., Soares, D.J., da Silva, J.Y.G., Benjamin, S.R., Guedes, M.L.F., 2019. Carnauba wax uses in food – A review. *Food Chem.* 291, 38–48.
- Gan, J., Lin, Q., Huang, Y., Wu, Y., Yu, W., 2023. Full-wood utilization strategy toward a directional luminescent solar concentrator. *ACS Nano* 17, 23512–23523.
- Giesbers, M., Marcelis, A.T.M., Zuillhof, H., 2013. Simulation of XPS C1s Spectra of organic monolayers by quantum chemical methods. *Langmuir* 29, 4782–4788.
- Gu, J.-w., Zhang, G.-c., Dong, S.-l., Zhang, Q.-y., Kong, J., 2007. Study on preparation and fire-retardant mechanism analysis of intumescent flame-retardant coatings. *Surface and Coatings Technology*, 201, 7835–7841.
- He, Z., Qian, J., Qu, L., Yan, N., Yi, S., 2019. Effects of Tung oil treatment on wood hygroscopicity, dimensional stability and thermostability. *Ind. Crops Prod.* 140, 111647.
- Humar, M., Lesar, B., 2013. Efficacy of linseed- and tung-oil-treated wood against wood-decay fungi and water uptake. *Int. Biodeterior. Biodegrad.* 85, 223–227.
- Janesch, J., Arminger, B., Gindl-Altmutter, W., Hansmann, C., 2020. Superhydrophobic coatings on wood made of plant oil and natural wax. *Prog. Org. Coat.* 148, 105891.
- Kapridaki, C., Maravelaki-Kalaitzaki, P., 2013. TiO₂-SiO₂-PDMS nano-composite hydrophobic coating with self-cleaning properties for marble protection. *Prog. Org. Coat.* 76, 400–410.
- Lesar, B., Pavlič, M., Petrič, M., Škapin, A.S., Humar, M., 2011. Wax treatment of wood slows photodegradation. *Polym. Degrad. Stab.* 96, 1271–1278.
- Li, J.H., Hong, R.Y., Li, M.Y., Li, H.Z., Zheng, Y., Ding, J., 2009. Effects of ZnO nanoparticles on the mechanical and antibacterial properties of polyurethane coatings. *Prog. Org. Coat.* 64, 504–509.
- Liu, Y., Li, L., Zhao, A., Song, X., Wei, L., Fang, M., Zheng, C., Zhu, X., 2024. Sustainable fragrance release wax oil coating for wood substrate based on peppermint essential oil microcapsules. *Ind. Crops Prod.* 208, 117848.
- Nurul Syahida, S., Ismail-Fitry, M.R., Ainun, Z.M.Aa, Nur Hanani, Z.A., 2020. Effects of palm wax on the physical, mechanical and water barrier properties of fish gelatin films for food packaging application. *Food Packag. Shelf Life* 23, 100437.
- Nykter, M., Kymäläinen, H.R., Gates, F., 2006. Quality characteristics of edible linseed oil. *Agric. Food Sci.* 15, 402–413.
- Ou, J., Zhang, M., Liu, H., Zhang, L., Pang, H., 2015. Matting films prepared from waterborne acrylic/micro-SiO₂ blends. *J. Appl. Polym. Sci.* 132.
- Pandey, K.K., 1999. A study of chemical structure of soft and hardwood and wood polymers by FTIR spectroscopy. *J. Appl. Polym. Sci.* 71, 1969–1975.
- Pandey, K.K., Pitman, A.J., 2003. FTIR studies of the changes in wood chemistry following decay by brown-rot and white-rot fungi. *Int. Biodeterior. Biodegrad.* 52, 151–160.
- Peng, Y., Wang, Y., Chen, P., Wang, W., Cao, J., 2020. Enhancing weathering resistance of wood by using bark extractives as natural photostabilizers in polyurethane-acrylate coating. *Prog. Org. Coat.* 145, 105665.
- Piao, X., Zhao, Z., Guo, H., Wang, Z., Jin, C., 2022. Improved properties of bamboo by thermal treatment with wood wax oil. *Colloids Surf. A: Physicochem. Eng. Asp.* 643, 128807.
- Ragunathan, T., Husin, H., Wood, C.D., 2020. Effects of crude palm oil and crude palm kernel oil upon wax inhibition. *ACS Omega* 5, 19342–19349.
- Rosu, L., Varganici, C.-D., Mustata, F., Rusu, T., Rosu, D., Rosca, I., Tudorachi, N., Teacă, C.-A., 2018. Enhancing the thermal and fungal resistance of wood treated with natural and synthetic derived epoxy resins. *ACS Sustain. Chem. Eng.* 6, 5470–5478.
- Schindler, M., Hawthorne, F.C., Freund, M.S., Burns, P.C., 2009. XPS spectra of uranyl minerals and synthetic uranyl compounds. II: the O 1s spectrum. *Geochim. Et. Cosmochim. Acta* 73, 2488–2509.
- Schönemann, A., Edwards, H.G.M., 2011. Raman and FTIR microspectroscopic study of the alteration of Chinese tung oil and related drying oils during ageing. *Anal. Bioanal. Chem.* 400, 1173–1180.
- Schwanninger, M., Rodrigues, J.C., Pereira, H., Hinterstoisser, B., 2004. Effects of short-time vibratory ball milling on the shape of FT-IR spectra of wood and cellulose. *Vib. Spectrosc.* 36, 23–40.
- Singh, T., Singh, A.P., 2012. A review on natural products as wood protectant. *Wood Sci. Technol.* 46, 851–870.
- Tang, C.C., Li, Y., Buzoglu Kurnaz, L., Li, J., 2021. Development of eco-friendly antifungal coatings by curing natural seed oils on wood. *Prog. Org. Coat.* 161, 106512.
- Traoré, M., Kaal, J., Martínez Cortizas, A., 2016. Application of FTIR spectroscopy to the characterization of archeological wood. *Spectrochim. Acta Part A: Mol. Biomol. Spectrosc.* 153, 63–70.

- Tulloch, A.P., 1971. Beeswax: Structure of the esters and their component hydroxy acids and diols. *Chem. Phys. Lipids* 6, 235–265.
- Ullah, K., Ahmad, M., Sofia, Qiu, F., 2015. Assessing the experimental investigation of milk thistle oil for biodiesel production using base catalyzed transesterification. *Energy* 89, 887–895.
- Varganici, C.-D., Rosu, L., Rosu, D., Mustata, F., Rusu, T., 2021. Sustainable wood coatings made of epoxidized vegetable oils for ultraviolet protection. *Environ. Chem. Lett.* 19, 307–328.
- Wexler, H., 1964. Polymerization of drying oils. *Chem. Rev.* 64, 591–611.
- Xia, Y., Yan, X., 2024. Preparation of UV topcoat microcapsules and their effect on the properties of UV topcoat paint film. *Polymers* 16, 1410.
- Zhang, H., Gan, J., Wu, Y., Wu, Z., 2023. Biomimetic high water adhesion superhydrophobic surface via UV nanoimprint lithography. *Appl. Surf. Sci.* 633, 157610.
- Zhang, D., Song, K., 2024. Effects of photoinitiators on curing performance of wood wax oil coating on wood. *Coatings* 14, 2.
- Zou, Y., Pan, P., Zhang, N., Yan, X., 2024. Effect of nano-silver solution microcapsules mixed with rosin-modified shellac microcapsules on the performance of water-based coating on Andoung wood (*Monopetalanthus* spp.). *Coatings* 14, 286.